Monitoring, Control System Development, and Experimental Validation for a Novel Extrapulmonary Respiratory Support Setup

Mahsa Doosthosseini, Kevin R. Aroom, Majid Aroom, Melissa Culligan, Warren Naselsky, Chandrasekhar Thamire, Henry W. Haslach, Jr., Stephen A. Roller, James Richard Hughen, Joseph S. Friedberg, Jin-Oh Hahn, Hosam K. Fathy*

***Abstract*—This paper presents a novel mechatronic setup intended for providing respiratory support to patients suffering from pulmonary failure. The setup relies upon the circulation of an oxygenated perfluorocarbon (PFC) through the abdominal cavity. Such circulation provides a potential pathway for the transport of oxygen to the bloodstream. However, the viability of this technology for CO_2 clearance has not been established. Moreover, there is a lack of experimental data enabling the modeling and identification of the underlying dynamics of this technology. To address these gaps, we develop a flexible experimental perfusion setup capable of monitoring and controlling key variables such as perfusate flowrate, temperature, pressure, and oxygenation. One important scientific objective of this setup is to enable the measurement of the impact of abdominal PFC perfusion on CO_2 clearance. The paper (i) summarizes the design of this setup; (ii) highlights the degree to which its data acquisition system enables the collection and cross-correlation of both perfusion-related and physiological variables; and (iii) discusses the development of flow, pressure, and temperature control algorithms for the setup. Experiments with large animals (swine) show that perfusion can potentially affect both O_2 and CO_2 dynamics, and that the setup succeeds in recording key data needed for modeling these dynamics.**

I. Introduction

This paper addresses the need for the integrated monitoring and control of a novel setup that can augment respiration without interfacing with the blood stream or utilizing the lungs. The setup is intended to address the societal need for providing pulmonary-independent life support to patients with respiratory failure. Respiratory failure is a life-threatening condition whose causes include acute respiratory distress syndrome (ARDS), pulmonary embolism, pneumonia, toxic inhalation, COVID-19 infection, etc. The fact that the U.S. alone has historically seen more than 100,000 ARDS-related hospitalizations annually, even during pre-pandemic years, highlights the public health magnitude of acute pulmonary failure [1].

The main functions of the respiratory system are to bring oxygen into the body and expel CO_2 out of the body. If either of these two functions, oxygenation or CO_2 removal, falls below critical levels, then the patient will not survive without additional support. If the condition is severe, then the patient will require mechanical ventilation. This is a technique where the airway is intubated to provide positive pressure assistance of the lungs. A potential complication of mechanical ventilation is barotrauma to the lungs [2], which can result in ventilator-induced lung injury (VILI) [3]. VILI can compound the underlying lung dysfunction and exacerbate the pulmonary failure – potentially to a fatal degree. In such situations, unless gas exchange is augmented by extra-pulmonary means, the patient will not survive.

Extra-corporeal membrane oxygenation (ECMO) is currently the only pulmonary-independent modality available to supplement gas exchange. It involves drawing blood out of the patient through a vascular cannula, oxygenating it, then pumping it back into the patient through another cannula [4]. Unfortunately, ECMO is an expensive resource, with one study indicating a mean total hospital cost above $200,000 per patient [5]. The availability of ECMO is limited by cost and personnel requirements: its initiation is typically performed by specially trained cardiac surgeons, and its maintenance requires constant monitoring by highly trained personnel. Even when available, ECMO is accompanied by contraindications or exclusion criteria that may make it a nonviable option for patients with potentially reversible lung failure [6]. Therefore, there is a need for additional ways to support respiration that do not require the lungs or ECMO.

The main idea motivating this paper is to supplement gas exchange by perfusing (i.e., circulating) an oxygenated perfluorocarbon (PFC) through a patient's peritoneal (i.e., abdominal) cavity. Perfluorocarbons (PFCs) are organic compounds consisting either predominantly or entirely of carbon and fluorine [7]. They are inert and recognized for their very high oxygen and carbon dioxide solubilities [8], [9]. Thanks to these properties, PFCs are well-suited for medical applications [10], including their use as blood substitutes [11]

The authors are with the Departments of Mechanical Engineering and Biomedical Engineering at the University of Maryland, College Park, and the University of Maryland School of Medicine in Baltimore, MD, USA. Emails: (mdoostho, karoom, maroom)@umd.edu, (MCulligan, WNaselsky)@som.umaryland.edu, (cthamire, haslach)@umd.edu, (stephen.a.roller, richardhughen)@gmail.com, JFriedberg@som.umaryland.edu, (jhahn12, hfathy)@umd.edu (Phone:+1 301-405-6617)

*Corresponding author.

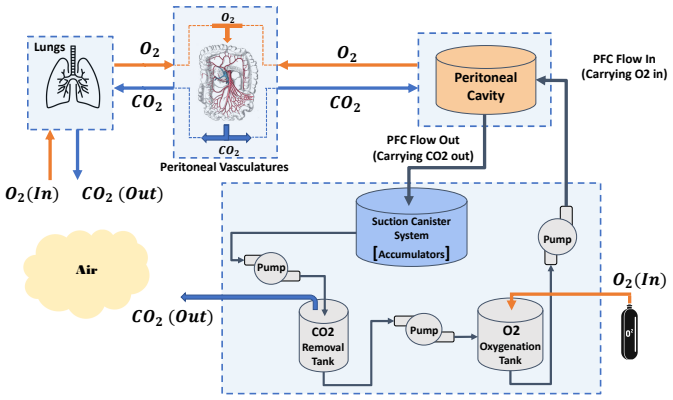

Fig. 1. Schematic of the third lung concept

as well as their use in ophthalmologic surgeries [12]. One particularly relevant application is the use of PFCs for *liquid ventilation*, or "liquid breathing" [13]. This refers to filling the lungs with an oxygenated PFC in an effort to augment gas exchange. Both laboratory studies and clinical trials have been performed on liquid ventilation, in patient and laboratory animal populations as diverse as premature infants [14], adults [15], and laboratory swine [16]. These studies show that while liquid ventilation does have the potential to supplement gas exchange [17], its benefits may not justify its adoption as an alternative to mechanical ventilation [18].

The research in this paper is similar to liquid ventilation in its use of PFC to augment gas exchange, but fundamentally distinct in its use of the abdominal cavity, as opposed to the lungs, for gas exchange. Figure (1) summarizes this respiratory support approach. A perfusion circuit is used for oxygenating PFC, removing CO_2 from it, and warming it to body temperature. The oxygenated PFC is then perfused through the abdomen, where processes such as diffusion allow it to exchange oxygen and CO_2 with the bloodstream. Finally, the PFC is drained out of the abdomen, potentially using negative pressure from a suction/vacuum pump. The end result is an approach that allows the peritoneal cavity to be used "like a lung," analogous to its use "like a kidney" for peritoneal dialysis [19]. One possible benefit of this "third lung" concept is its potential to provide pulmonary-independent gas exchange supplementing mechanical ventilation, thereby resting the lungs and helping them heal. Another potential benefit is the fact that the third lung innovation does not require a direct blood-device interface, thereby avoiding many of the risks and contra-indications of ECMO.

Previous medical research by one of this paper's co-authors (Friedberg) shows that the third lung concept is indeed effective at providing oxygenation to large hypoxic animal models (namely, laboratory swine) [20]. While this prior research is encouraging, it leaves at least four important open questions and research challenges. First, it is not clear what operating conditions (e.g., perfusion flowrates, pressures, temperatures, PFC oxygenation levels, etc.) are ideal for the third lung concept. Second, the impact of the third lung intervention on hemodynamic variables such as heart rate has yet to be fully characterized. Third, the impact of the intervention on CO_2 clearance has not yet been examined in the literature. Fourth, there is a need to implement the third lung concept using a mechatronic setup with extensive data acquisition and control capabilities enabling the scientific examination of the above three questions. Particularly relevant to this paper is the question of whether PFC perfusion can potentially affect the dynamics of CO_2 clearance. Thus, the main scientific goal of the paper is to present a mechatronic setup that can, for the first time, address the following question: *does abdominal PFC perfusion have the potential to result in a measurable difference in CO_2 dynamics in laboratory swine?*

The remainder of this paper presents the above mechatronic setup, focusing on its monitoring and control capabilities, and is organized as follows. Section II summarizes the setup's mechanical design. Section III describes the setup's monitoring and data acquisition system. Section IV summarizes the setup's key closed-loop control functionalities. Section V presents preliminary data from laboratory animal experiments highlighting some of the setup's successes in controlling perfusion parameters such as perfusate flowrate, temperature, pressure, and oxygenation level. Finally, Section VI summarizes the paper's conclusions.

II. Design of the Third Lung Ventilator

Experiments on the third lung intervention have, to date, focused on large laboratory animals (swine) because of proximity in size, core body temperature, and ventilation needs to human patients. The perfusion setup described in this paper is designed to facilitate these experiments, with the ultimate goal of enabling emergency interventions in human patients. The traditional process for designing such a setup involves *(i)* identifying potential users of the setup (e.g., medical professionals), *(ii)* interviewing these users, *(iii)* creating a list of functional requirements based on these interviews, *(iv)* exploring different conceptual designs meeting these requirements, *(v)* selecting a conceptual design, and finally *(vi)* iterating through the setup's conceptual, preliminary, and detailed designs. This section summarizes the *(i)* **functional requirements** for the setup, as well as the *(ii)* **design solutions** adopted for each functional requirement. The paper's authors explored multiple design solutions for each functional requirement, as discussed for some of the key functional requirements below. The setup is specifically designed to meet five main high-level functional requirements, namely:

1) Oxygenating the PFC and removing CO_2 from it prior to perfusion.
2) Providing a PFC perfusion flowrate sufficient for supplementing gas exchange. For large animal experiments, prior research suggests that flowrates of up to 6 liters per minute may potentially be required [20].
3) Delivering up to 11 liters of PFC to the abdomen at any given time. This is important, considering the degree to which the abdominal cavity distends during perfusion.

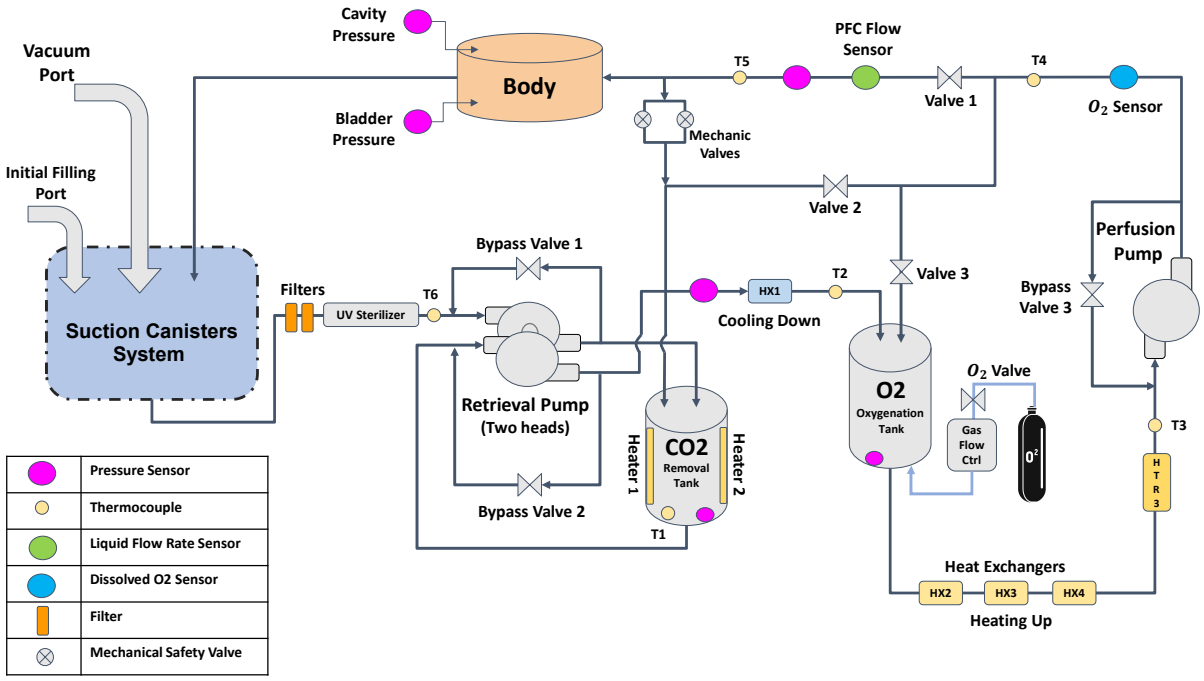

Fig. 2. The third lung ventilator setup diagram

Filling the distended abdomen of a $40-50\ kg$ adult pig, for example, can potentially consume 6-7 liters of PFC.

4) Achieving perfusion temperatures that are consistent with core body temperature - namely, $37°C$ for human patients and $39°C$ for laboratory pigs.
5) Ensuring safety by avoiding intra-cavity pressures conducive to intra-abdominal hypertension and/or compartment syndrome.

Figure (2) presents the design of the third lung setup, tailored to meet the above requirements. When filled, the setup can accommodate 22-26 liters of PFC, of which up to 11 liters can be supplied to the animal's or patient's body at any time. The remaining PFC must stay in the setup to ensure that the setup is properly primed and able to sufficiently oxygenate the PFC. PFC enters and leaves the abdomen through tubes typically used as central venous catheters. Different catheter sizes can be accommodated, a typical size being 36 on the French scale (i.e., 12 *mm*). An oxygenated PFC (specifically, a mix of cis- and trans-Perfluorodecalin) is perfused through the abdomen of the patient or animal. The PFC then drains into an accumulator using a combination of gravitational drainage and active suction via a vacuum pump. Two different versions of this accumulator have been built and can be rapidly interchanged, namely: a single-canister system and the dual-canister system in Fig. (3). The former system uses one canister to receive fluid drained from the test animal and supply it to the rest of the setup. In contrast, the dual-canister system switches periodically between a canister that recovers fluid from the animal versus a canister from which fluid is pumped into the rest of the setup.

Once the fluid is recovered by the accumulator system,

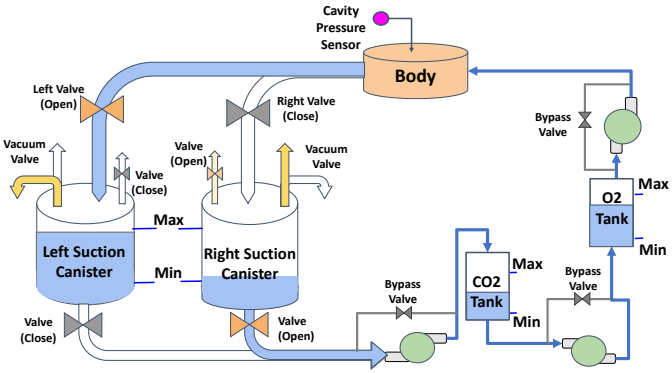

Fig. 3. The two-canister accumulator system

it is filtered then exposed to an ultraviolet flood light. The fluid then passes through a chamber where CO_2 is purged. The specific setup sketched in Fig. (2) uses PFC heating plus exposure to an oxygen stream as means of CO_2 removal, the idea being to rapidly achieve equilibrium between dissolved and incoming gas concentrations. Alternative CO_2 removal mechanisms include the use of vacuum to bubble CO_2 out of the PFC as well as the use of chemical removal means (e.g., soda lime canisters). If the temperatures used for CO_2 removal exceed the ideal perfusion temperature, the setup provides the option to pass the warm PFC through a heat exchanger connected to cold water flow from a cardioplegic heater/chiller. The PFC is then oxygenated using a gas bubble chamber connected to an oxygen tank through an actively-controlled valve, with the possibility that future designs may

employ membrane gas exchangers instead. Next, the temperature of the PFC is regulated to meet the desired perfusion target using a mix of electric heating and heat exchange with hot water from the cardioplegic heater/chiller unit. Finally, the oxygenated PFC is pumped into the abdomen.

As shown in Fig. (2), the setup needs to transfer PFC from the suction canisters to the CO_2 removal chamber, then to the oxygenation chamber, then finally to the abdomen. Two peristaltic pumps are used for achieving these three functionalities. A dual-head "retrieval pump" transfers fluid from the suction canister(s) to the CO_2 removal chamber, then to the oxygenation chamber. Next, a "perfusion pump" supplies PFC to the animal. Balancing the PFC fluid levels in the various chambers can be achieved through bypass valves, as shown in Fig. (2), with the recognition that modifying the setup to incorporate three independent pumps may potentially provide greater control authority. The setup incorporates a mix of spring-loaded passive and actively-controlled mechanical bypass valves on the final perfusion line. These valves provide the ability to bypass the abdomen if intra-cavity pressure increases beyond critical limits dictated by setup design (in case of the passive valves) or operator input, if the operator dictates a software-based pressure limit (in case of the active valves). This is important for avoiding cavity pressures conducive to compartment syndrome.

Temperature control is potentially critical for the success of the third lung intervention, and requires significant fluid heating capabilities. Heating is needed for ensuring compatibility between perfusion temperature and core body temperature. Heating beyond core body temperature is also potentially important for CO_2 removal. For illustrative purposes, consider the problem of heating the PFC from a room temperature of $22°C$, to a desired CO_2 removal temperature of $42°C$, assuming a PFC flowrate of 5 liters per minute. Knowing that the density, ρ, of Perfluorodecalin is $1.93\ kg/L$ and its specific heat capacity, C_p, is $1000\ J\ kg^{-1}\ K^{-1}$, Eq. (1) solves for the heat, Q_{th}, required for this functionality[1]:

$$Q_{th} = \dot{m} C_p \Delta T = 5 \times 1.93 \times 100 \times 20 \cong 3216\ W, \quad (1)$$

where ΔT is the desired rise in PFC temperature and $\dot{m}$ is the mass flowrate of PFC.

The setup is equipped with two $250\ W$ electric heaters in its CO_2 removal chamber plus a $100\ W$ electric heater attached to the final perfusion line. Moreover, the setup is connected through heat exchangers to the hot and (optionally) cold water outputs of a cardioplegic chiller/heater unit. The chiller/heater unit can provide up to $3000\ W$ of heat to its output hot water, which can be raised to temperatures as high as $41°C$. Given the proximity of this hot water temperature to the final perfusion temperature, three of the setup's four heat exchangers are used for heating the PFC, compared to a single optional heat exchanger for cooling.

[1]Note: this computation neglects convective loss and assumes that fluid temperature attains the desired change in a single pass through the setup.

These details highlight the importance of the coordinated control of the setup's heating (and potential cooling) assets in order to ensure effective perfusion temperature control. Other critical variables that the setup must monitor and control include perfusion flowrate, total perfused volume, perfusate gas concentrations, and intra-cavity pressure. The remainder of this paper presents a detailed description of the monitoring, data acquisition, and control functionalities implemented to meet these goals.

III. Setup monitoring and data acquisition

Figure (4) provides a high-level overview of the components of the setup's monitoring and data acquisition system. This system: (i) monitors the setup's performance, (ii) monitors the effect of perfusion on the test animal, and (iii) enables important closed-loop control functionalities. Up to 160 signals are collected by this system, from 28 different sensors and patient monitors, in order to collectively satisfy the data acquisition requirements below. The physical locations of these sensors are indicated in Fig. (2-3).

- **Fluid height/volume monitoring** (10 sensors, 10 signals): The setup has the ability to monitor the height of the PFC in all of its canisters - namely, the oxygenation canister, the CO_2 removal canister, and its 1-2 canister accumulator. This is achieved by measuring the difference between the air/suction pressure at the top of each canister versus the fluid pressure at the bottom of the canister. The setup is also equipped with a redundant/second fluid height/volume system using 4 fluid level sensors.
- **PFC flowrate monitoring** (1 sensor, 1 signal): The setup monitors perfusion using a PFC flowrate sensor.
- **Oxygen flowrate monitoring** (2 sensors, 2 signals): The setup monitors the rate at which oxygen flows into the CO_2 removal tank using a gas mass flowrate sensor. This rate is adjusted using a manual valve. The setup also controls oxygen flowrate into its oxygenation chamber using an active gas flowrate controller. This controller provides a measurement of the achieved oxygen flowrate back to the setup's data acquisition system.
- **Oxygen concentration monitoring** (2 sensors, 2 signals): Optical sensors are mounted on both the animal inflow and outflow lines in order to monitor the concentration of dissolved oxygen in the PFC.
- **Fluid temperature monitoring** (6 sensors, 6 signals): Thermocouples are used for monitoring PFC temperatures at multiple points in the setup, namely: (i) the CO_2 removal tank; (ii) the inlet of the oxygenation tank; (iii) the inlet of the perfusion pump; (iv) the outlet of the perfusion pump; (v) the final tube in the setup prior to perfusion; and (vi) the surface of the polishing heater.
- **Perfusion pressure monitoring** (4 sensors, 4 signals): The setup has the ability to measure the test animal's abdominal intra-cavity pressure and bladder pressure through two catheter-mounted pressure sensors. The

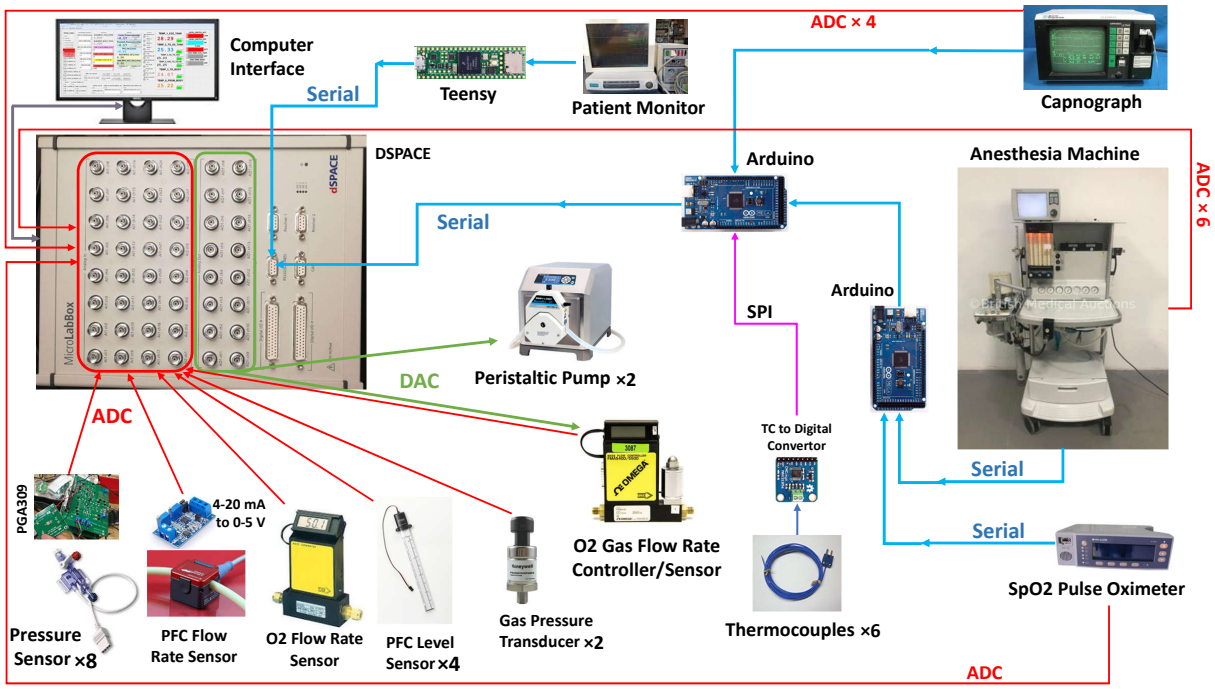

Fig. 4. Setup monitoring and data acquisition system

setup uses two additional pressure sensors for mc ing internal fluid pressures prior to perfusion.

- **Physiological signal monitoring** (4 monitors, 1 nals): The setup interfaces with four medical moni systems in order to collect data regarding th animal's physiological state (e.g., hemodynamics response to perfusion. Specifically, the setup can face with: (i) a Nellcor **pulse oximeter**; (ii) a Capr **capnograph**; (iii) a Penlon **anesthesia machine** (iv) a TRAM-RAC **patient monitor**. Collectively, devices provide 19 different measurements, with of these measurements providing an important c of redundnacy (including, for example, two dif measurements of pulse oximetry).

The setup's monitoring and control system is built around a central data acquisition board - in this case, a dSpace MicroLabBox II board often used for instrumentation and control research [21]–[23]. All analog sensor/monitor signals are read directly by the dSpace board. For sensor signals that use a current-based (i.e., $4 - 20\ mA$) analog communication protocol, standard integrated circuits are used for converting the signals to a voltage-based protocol first, prior to dSpace-based data acquisition. The remaining signals are communicated using either the RS-232 serial protocol or the serial peripheral interface (SPI) protocol, with TTL/RS-232 signal level conversions implemented as/when needed. Two Arduino Mega 2560 boards, together with a Teensy board (an Arduino clone) are used for reading these non-analog signals, as shown in Fig. 4. This multiplicity of data acquisition boards has made it possible to prototype the overall data acquisition rapidly, for the purposes of

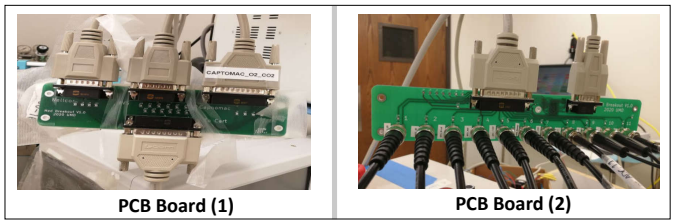

Fig. 5. Medical equipment communication boards

laboratory research, with the understanding that a single-board solution is potentially more attractive for technology commercialization. The setup collects the signals from all the medical devices using a custom printed circuit board (PCB), as shown on the left hand side of Fig. (5). A second PCB, shown on the right hand side of Fig. (5) is used to input these signals into the Arduino and dSpace boards.

Different components of the above data acquisition system monitor different underlying dynamics, with significantly different associated time constants. For example, if any of the setup's tubes are pinched during an experiment, the dynamics of the associated rise in fluid pressure are likely to be much faster than the dynamics of animal blood gas concentrations. With this in mind, the setup's dSpace board has a relatively fast master sampling time of $10\ ms$. Other components of the setup have progressively slower sampling rates and/or data processing times. For example: (i) The SPI protocol is used for reading temperatures every $100\ ms$. (ii) The Arduino boards communicate data to the dSpace board every $150\ ms$. (iii) The Teensy board communicates data to

the dSpace board every 500 ms. (iv) The pulse oximeter, anesthesia machine, and patient monitor communicate data to the Arduino and Teensy boards every 2000 ms. (v) The capgnograph communicates data to the corresponding Arduino board every $10,000$ ms. (vi) Finally, the oxygen sensors update their readings every 60 seconds, saving them to a local file using (proprietary) standalone software.

The above setup requires four calibration efforts on a regular basis, potentially once per animal experiment, namely.

- Calibrating the PFC **flowrate sensor** by using the setup to pump a known volume of fluid into an external tank, then calibrating the sensor's software to ensure that the time integral of its flowrate measurement matches the volume of fluid delivered.
- Calibrating the **canister pressure-based fluid height sensors** by filling the canisters to known fluid heights, then adjusting the reference voltage outputs of these sensors to match these known heights.
- Calibrating the **cavity and bladder pressure sensors** at the beginning of each animal experiment by exposing them sensors to atmospheric pressures, then adjusting the reference voltage outputs of these sensors to furnish a correct reading of atmospheric pressure.
- Calibrating the **dissolved oxygen concentration sensors.** To achieve this for the inflow sensor, two samples of PFC were prepared with dissolved oxygen concentrations corresponding to partial oxygen pressures of 159 $mmHg$ and 760 $mmHg$, respectively, at room temperature. These samples were then mixed in different proportions in order to prepare PFC samples with intermediate oxygen partial pressures. The sensor's reading was then correlated to dissolved oxygen fraction. Figure (6) shows the resulting calibration plot.

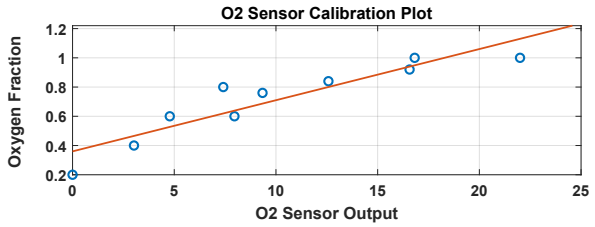

Fig. 6. Calibration plot for optical oxygen sensor

IV. Setup Control

Four closed-loop control functionalities are implemented in the setup as discussed below, building on well-established principles from fields such as fluid power control [24]. Specifically, the setup contains discrete-event algorithms to control: (i) the filling of the two-canister system when in use; and (ii) the filling of the CO_2 removal chamber and oxygenation chambers. The setup also contains proportional-integral (PI) algorithms for controlling (iii) the temperatures of the PFC in the CO_2 removal chamber and final perfusion line; and (iv) the final perfusion flowrate/pressure.

1- Multi-Canister Switching Control

The intent of the dual-canister accumulator is to enable fluid to be simultaneously *(i)* drained from the test animal via active suction and *(ii)* delivered to the setup through the retrieval pump, with minimal overlap between these two functionalities. Fig. (7) summarizes the discrete-event logic used for achieving this goal. The figure generalizes this algorithm to an N-canister system. Most of the time, the setup is in a "k-filling" state, where canister k is being filled and all other canisters are being emptied. When canister k is full or any other canister is empty, an immediate switch takes place to a "transitioning" state. This state persists for a fixed duration of time, during which the retrieval pump is shut down, suction is applied to the next canister in the sequence of canisters to fill, fluid is routed to that new canister, and the retrieval pump is restarted. Once this transition is complete, the discrete-event control algorithm automatically moves to a state where it is filling the next canister in the filling sequence, namely, canister number $(k+1) mod N$.

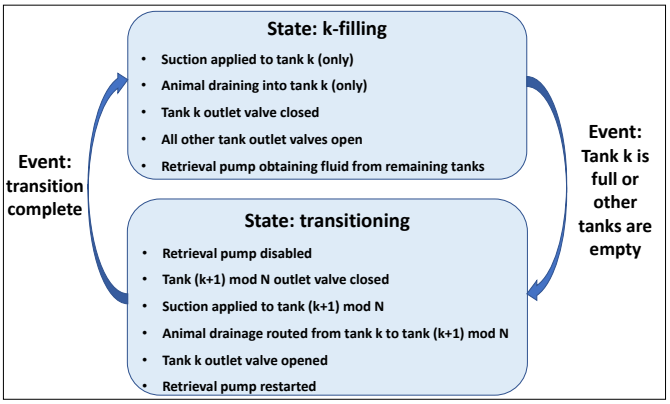

Fig. 7. Multi-canister switching control algorithm

2- Control of Oxygenation and CO_2 Chamber Filling

Three different control algorithms/loops are used for controlling the retrieval pump and its associated bypass valves. Collectively, these loops ensure that the oxygenation and CO_2 removal chambers are replenished with fluid whenever possible, but prevented from overfilling.

- The first loop controls the retrieval pump flowrate. During normal operation, this flowrate is set to a constant value. However, when both the oxygenation and CO_2 removal tanks are full or when all the canisters in the accumulator are empty, the pump enters a temporary shutdown state, where flowrate is set to zero. The pump dwells in this state for a fixed time duration, then returns to normal operation. This translates to a 2-state finite state machine governing the pump's operation, where it transitions automatically from normal operation to shutdown when needed.

- The second and third loops control the bypass valves for the first and second retrieval pump heads, respectively. These valves are closed during normal operation, allowing the retrieval pump to supply PFC from the accumulator to the CO_2 removal tank, then to the oxygenation tank. However, when the $CO2$ removal tank or oxygenation tank is full, the corresponding bypass valve automatically switches to a state where it is open, allowing flow to bypass the full tank. The valve dwells in this state for a fixed time duration, then automatically returns to the normal operation state. This makes it possible for the retrieval pump to replenish the above tanks without overfilling either of them.

3- PFC Temperature Control

Two different loops are used for controlling PFC temperature (i) in the CO_2 removal chamber and (ii) at the final perfusion point. Both loops rely on proportional integral (PI) control with saturation and anti-windup logic. In both cases, the dynamics of PFC temperature are assumed to be governed by the following simple energy balance:

$$\rho V C_p \dot{T} = \rho Q C_p (T_{in} - T) + hA(T_\infty - T) + uR_o I_o^2 \quad (2)$$

In the above equation, T is the PFC temperature in the given control volume, assumed to be equal to the control volume's outlet temperature. Depending on the control loop, this control volume is either the CO_2 removal chamber or the pipe section/manifold being heated by the final perfusion heater. The volume of PFC being heated is denoted by V. Moreover, the density and specific heat capacity of the PFC are denoted by ρ and C_p, respectively. Thus, the term $\rho V C_p \dot{T}$ equals the rate of change of thermal energy stored in the control volume, assuming that the amount of PFC in this control volume, V, is approximately constant. The first term contributing to this rate of change, $\rho Q C_p (T_{in} - T)$, equals the rate of energy transfer due to the flow of PFC, where Q is the volumetric flowrate of the PFC and T_{in} is the PFC temperature at the inlet of the control volume. The second term contributing to temperature change, $hA(T_\infty - T)$, represents the rate of convection heat transfer, where h is the heat transfer coefficient, A is the area exposed to convection, and T_∞ is ambient temperature. Finally, the term $uR_o I_o^2$ represents electric heating of the PFC, where R_o is the heater's effective resistance, I_o is the nominal current flowing through the heater when it is turned on, and u is an adjustable pulse width modulation (PWM) duty ratio for the heater. This PWM duty ratio is constrained to be between 0 and 1.

Fig. (8) shows the PI loop used for temperature control in the CO_2 removal chamber. The plant dynamics block in the figure represents Eq. (2). The difference, $E(s)$ between the desired reference temperature, $R(s)$, and actual temperature, $T(s)$, is passed through a PI controller, $k_p + k_I/s$, with a proportional gain k_p and integral gain k_I, to produce a PWM ratio $U'(s)$. This PWM ratio is then passed through a saturation function in order to ensure that the final commanded

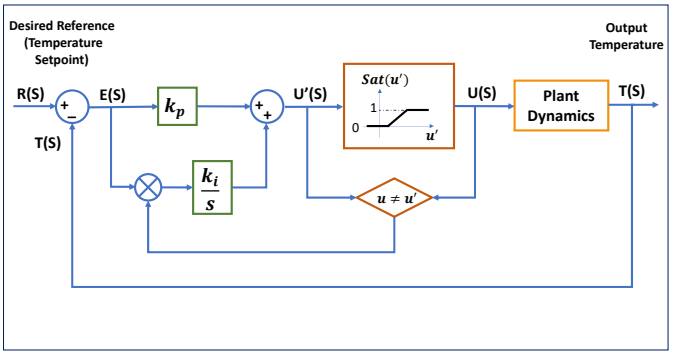

Fig. 8. Closed-loop temperature control

PWM ratio, $U(s)$, lies between 0 and 1. If the saturation function is active, meaning that there is a difference between the signals U' and U, then the integral feedback functionality is disabled (i.e., clamped) to prevent integrator windup. When the saturation function is inactive, the resulting closed-loop expression for the PFC temperature, $T(s)$, ensures ideal steady-state target temperature tracking in the presence of constant ambient and inflow temperature disturbances:

$$T(s) = \frac{\rho Q C_p T_{in} + hAT_\infty + (k_p s + k_I) R_o I_o^2 R(s)}{s(\rho C_p (Vs + Q) + hA) + (k_p s + k_I) R_o I_o^2} \quad (3)$$

Temperature control for the CO_2 removal chamber was tuned by fitting the open-loop dynamics of Eq. (2) to an experimental step response test, then using classical pole placement to set the gains k_p and k_I. A similar process was used for tuning the gains of the final perfusion temperature controller, with one important caveat compared to the CO_2 chamber temperature controller. Specifically, because the final perfusion heater is mounted directly on a metal pipe carrying PFC, as opposed to being immersed in a canister containing PFC, it is significantly more vulnerable to overheating. This vulnerability is particularly noticeable for small or zero PFC flowrates. This effect can be seen by examining the sensitivity of the above closed-loop temperature dynamics to errors in the flowrate, Q, assuming a small fluid volume, V. To address this, the perfusion heater's controller contains an additional term that brings the corresponding PWM ratio to zero if the temperature of the final perfusion heater exceeds $55°C$. When this function is activated, integral control is disabled (i.e., clamped) to prevent windup.

4- Perfusion Flowrate and Pressure Control

The final perfusion controller dictates the flowrate command to the perfusion pump. The controller is designed to ensure steady-state tracking of a user-defined desired perfusion flowrate during normal operation, while ensuring safe perfusion pressures. The controller outputs a flowrate command, $Q'(t)$, related to a user-defined desired flowrate $Q_{des}(t)$ as follows:

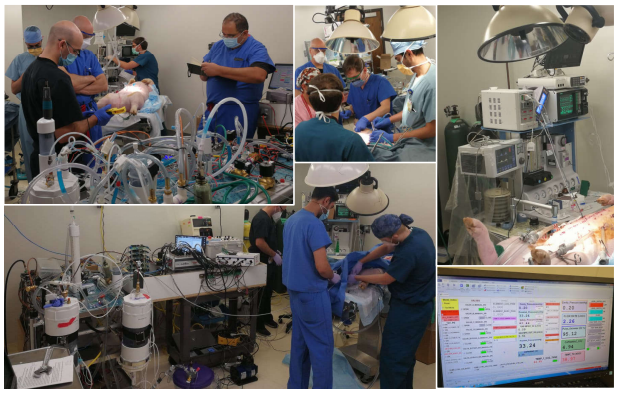

Fig. 9. The first and second animal experiment

$$
\begin{aligned}
Q'(t) &= k_{ff} Q_{des}(t) \\
&+ I(t) k_q \int_0^t (Q_{des}(\tau) - Q_{meas}(\tau)) d\tau \\
&+ (1 - I(t)) k_c \int_0^t (P(\tau) - P_{set}) d\tau
\end{aligned} \tag{4}
$$

In the above control law, $P(t)$ denotes peritoneal cavity pressure, and P_{set} is a user-defined pertioneal cavity setpoint pressure that should ideally not be exceeded for prolonged time durations. A dimensionless indicator function, $I(t)$, is defined as equalling 1 when $P(t) > P_{set}$, and equalling 0 otherwise. The volumetric flowrate, $Q'(t)$, is governed by three terms: a feedforward term $k_{ff} Q_{des}(t)$ that allows for open-loop control calibration, plus two integral feedback terms. The controls gains for these three terms are denoted by $k_f f$ (dimensionless) for the feedforward gain, k_q (units: s^{-1}) for the integral flowrate correction gain, and k_c (units: $m^3 Pa^{-1} s^{-2}$) for the integral pressure correction gain. Only one of the above integral feedback terms is active at any given time. When peritoneal cavity pressure exceeds the setpoint pressure, an integral controller with a gain k_c is used for bringing cavity pressure down to the setpoint. In contrast, when peritoneal cavity pressure is below the setpoint, an integral controller with a gain k_q is used for matching the true perfusion flowrate measured by the flowrate sensor, $Q_{meas}(t)$, to the desired flowrate dictated by the user.

The actual flowrate command communicated to the perfusion pump is equal to $Q'(t)$, with the exception of two extreme conditions. First, when the fluid level in the oxygenation tank drops below a certain minimum level, the perfusion pump controller enters a temporary discrete-event state where perfusate flowrate is curtailed by 50% while the oxygenation tank is replenished. Second, when cavity pressure exceeds a user-defined safety limit $P_{max} > P_{set}$, the perfusion pump controller enters a different temporary discrete-event state where perfusion is completely disabled.

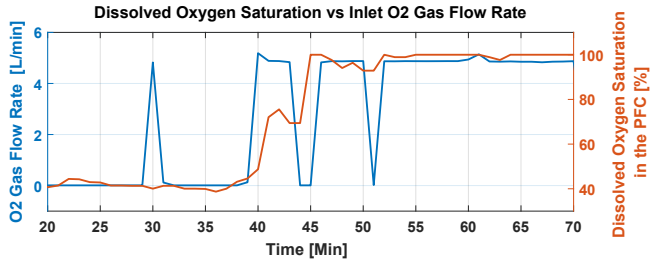

Fig. 10. Illustration of setup oxygenation performance

V. Results

Four animal experiments have been conducted to date, as illustrated in Fig. (9). These experiments employed different functionalities in the above setup. For example, the first animal experiment did not employ active suction for drainage of PFC from the test animal, whereas the next 3 animal experiments did. Moreover, the first two animal experiments employed a single-canister accumulator, whereas the third and fourth experiments predominantly employed a dual-canister accumulator. This section discusses the efficacy of the setup's data acquisition and control functionalities, from a mechatronics perspective. The section also highlights some of the core scientific lessons learned from the above four experiments. Six lessons pertaining to the setup s functionality are visible from experiments performed to date:

First, the setup is capable of rapidly oxygenating its stored Perfluorodecalin. Figure (10) illustrates this by plotting the open-loop commanded flowrate of oxygen into the oxygenation chamber (blue) and the resulting measured percentage of dissolved oxygen in the PFC as a function of time (red), during one of the animal experiments. A rapid increase in dissolved oxygen percentage is achieved while the PFC is recirculated through the setup, in preparation for perfusion.

Second, the setup is capable of monitoring and controlling the temperature at which both CO_2 stripping and perfusion take place, as shown in Fig. (11). Good reference tracking is achieved for both temperatures, with a very small steady-

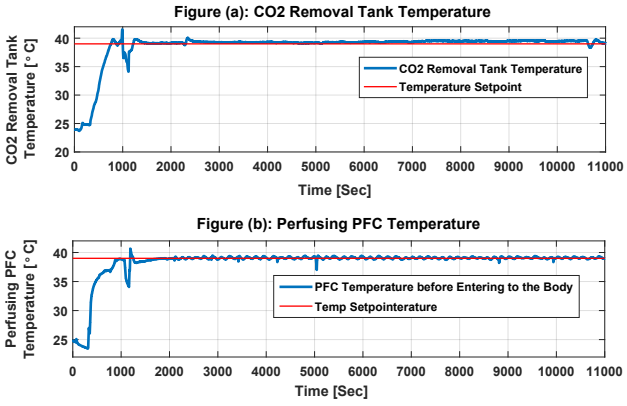

Fig. 11. CO2 removal tank and perfusing PFC temperatures (second animal experiment)

state CO_2 tank temperature error corresponding to slight overheating of the PFC.

Third, the setup is capable of both monitoring and controlling the final perfusion flowrate, in compliance with user input. Figure (12) illustrates this by comparing the commanded (blue) versus measured (red) PFC flowrate profiles during a portion of the third animal experiment. The setup was operated in manual flowrate control mode during this particular experiment, as opposed to automated control mode. Therefore, Fig. (12) illustrates successful feedforward control tuning, as opposed to successful steady-state flowrate command tracking through integral action.

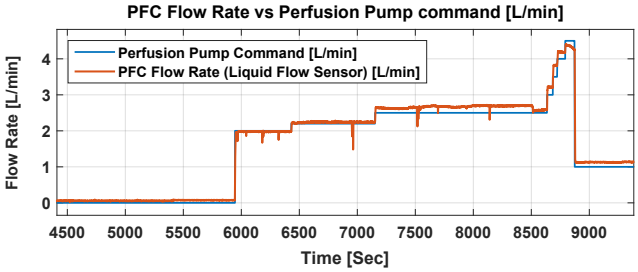

Fig. 12. Measured vs. commanded PFC flowrate (third animal experiment)

Fourth, the setup is capable of detecting and avoiding excessive peritoneal intracavity pressures. Fig. (13) illustrates this by plotting the setpoint cavity pressure (red) versus measured cavity pressure (blue) for a portion of the third animal experiment. Excursions beyond the setpoint pressure are brief. Moreover, they are followed by rapid curtailment of fluid flowrate (not shown), leading to rapid curtailment of cavity pressure. Negative pressures at the end of the plot are potentially indicative of the use of suction for fluid retrieval.

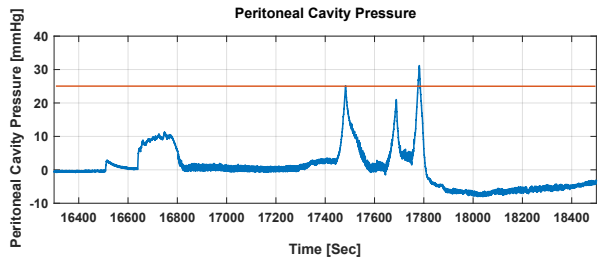

Fig. 13. The peritoneal cavity pressure measurement vs the pressure setpoint (Data from the third animal experiment)

Fifth, the setup provides sufficient data for assessing the viability of perfusion for oxygenating the test animal. Fig. (14) illustrates this by showing data from one animal oxygenation event. Specifically, the figure plots the animal pulse oximetry (blue) and PFC flowrate (red) versus time. The initial decline in pulse oximetry corresponds to a change in ventilator settings inducing hypoxia. Subsequent improvements in pulse oximetry may be due to a combination of physiological recovery by the animal and/or PFC perfusion. Analyzing

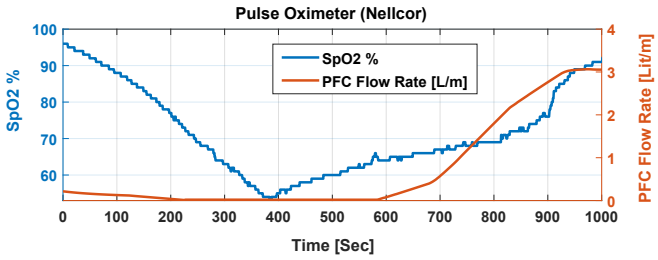

Fig. 14. Perfusate flowrate and pulse oximetry (second animal experiment)

the viability of perfusion for improving pulse oximetry is an open topic for ongoing research, exploiting this paper's setup. However, the figure shows that the setup is capable of measuring key variables that can be used for this analysis.

Finally, the setup provides sufficient data for assessing the viability of CO_2 removal from test animals. Fig. (15) illustrates this by plotting perfusion flowrate, inspired CO_2 concentration, and end-tidal CO_2 concentration for a portion of the second animal experiment. Hypercarbia is induced, in this case, through a reduction in minute ventilation. Improvements in end-tidal CO_2 concentration $(ETCO2)$ may be caused by physiological recovery mechanisms or perfusion, or a combination of both effects. Analyzing these different mechanisms is left open for ongoing research, building on the setup described in this paper. Please note that the setup's capnograph measures gas concentrations in a tracheal tube, and infers both inspired and end-tidal CO_2 concentrations from tracheal measurements. Therefore, changes in inspired gas concentration $(FICO2)$ measurements are likely to reflect gas mixing and re-breathing in the tracheal tube.

From a scientific perspective, the primary objective of this paper is to enable fundamental inquiry into the impact of peritoneal PFC perfusion on animal gas exchange dynamics. This is particularly important in the context of CO_2 clearance dynamics, which remain relatively unexplored in the context of peritoneal PFC perfusion in large laboratory animals. As shown in Fig.(15), the onset of perfusion coincides with a drop in end-tidal CO_2 partial pressure of more than 7 $mmHg$, within the span of approximately 300 seconds after the onset of perfusion. To the best of the authors' knowledge, this is the first result in the literature suggesting a drop in $ETCO_2$ concomitant with peritoneal PFC perfusion in large laboratory animals. Important fundamental scientific questions remain open for future research, such as: *(i)* whether this is a repeatable outcome, and under which conditions; *(ii)* whether this outcome can indeed be traced to a successful gas exchange mechanism representing CO_2 clearance from the test animal; and *(iii)* what statistical and/or clinical significance can potentially be attributed to this potential outcome. The goal of this paper is to present the data acquisition and control system of a mechatronic setup that enables inquiry into these questions, recognizing that the questions themselves remain open for future research.

VI. Conclusions and Future Work

This paper presents the development, design, and implementation of a peritoneal perfusion setup for studies on animal oxygenation using perfluorocarbons. The paper focuses on the setup's monitoring, data acquisition, and control capabilities as a mechatronics setup. Four animal experiments have been conducted to date using this setup. These experiments highlight the setup's functionalities from an engineering perspective. These functionalities include the ability to monitor and control perfusate flowrate, pressure, and temperature. The setup is also capable of simultaneously tracking both physical perfusion variables and physiological animal responses. The question of what factors affect the efficacy of peritoneal PFC perfusion as a gas exchange mechanism remain open for ongoing/future research. Moreover, the related question of the minimum viable level of setup complexity and sophistication for gas exchange also remains open for ongoing/future research. The design of the setup in this paper focuses predominantly on achieving a level of sophistication in data acquisition and control that is conducive to scientific exploration, recognizing that practical clinical implementation may benefit from setup simplification.

ACKNOWLEDGEMENTS

This research was conducted under IACUC #0121006 at The University of Maryland Medical School, Baltimore, MD (UMB). Support for this research was provided by the Mechanical Engineering Department at The University of Maryland (UMD), UMD startup funding for Dr. Hosam Fathy, an internal grant from The UMD Device Development Fund, and a National Science Foundation (NSF) EAGER grant to Dr. Hosam Fathy, Dr. Joseph Friedberg, and Dr. Jin-Oh Hahn (NSF CMMI Award #2031251, #2031245). Any Opinions, findings and conclusions or recommendations expressed in this material are those of the author(s) and do not necessarily reflect those of NSF. The majority of the setup's monitoring, data acquisition, and control functionalities were developed through NSF funding, with funding from other sources contributing to earlier hardware development. The authors gratefully acknowledge all of these sources of support. The authors also gratefully acknowledge the valuable support of other colleagues at UMD/UMB, including Grace Anyetei-Anum, Dr. Hyun-Tae Kim, Dr. Joshua Leibowitz, and Dr. Miao Yu.

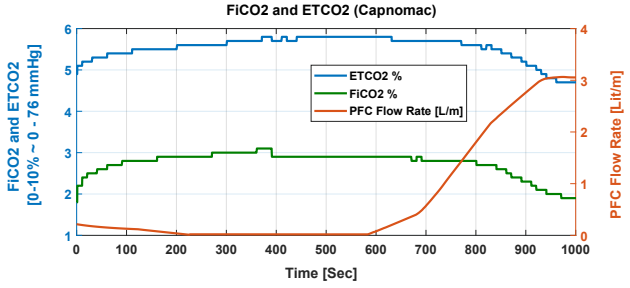

Fig. 15. Inspired and end-tidal CO_2 concentrations and perfusate flowrate (second animal experiment)

References

[1] E. Eworuke, J. M. Major, and L. I. G. McClain, "National incidence rates for acute respiratory distress syndrome (ards) and ards cause-specific factors in the united states (2006–2014)," *Journal of critical care*, vol. 47, pp. 192–197, 2018.

[2] A. Anzueto, F. Frutos-Vivar, A. Esteban, I. Alía, L. Brochard, T. Stewart, S. Benito, M. J. Tobin, J. Elizalde, F. Palizas *et al.*, "Incidence, risk factors and outcome of barotrauma in mechanically ventilated patients," *Intensive care medicine*, vol. 30, no. 4, pp. 612–619, 2004.

[3] M. Cressoni, M. Gotti, C. Chiurazzi, D. Massari, I. Algieri, M. Amini, A. Cammaroto, M. Brioni, C. Montaruli, K. Nikolla *et al.*, "Mechanical power and development of ventilator-induced lung injury," *Anesthesiology*, vol. 124, no. 5, pp. 1100–1108, 2016.

[4] M. Schmidt, D. Hajage, G. Lebreton, A. Monsel, G. Voiriot, D. Levy, E. Baron, A. Beurton, J. Chommeloux, P. Meng *et al.*, "Extracorporeal membrane oxygenation for severe acute respiratory distress syndrome associated with covid-19: a retrospective cohort study," *The Lancet Respiratory Medicine*, vol. 8, no. 11, pp. 1121–1131, 2020.

[5] V. Mishra, J. L. Svennevig, J. F. Bugge, S. Andresen, A. Mathisen, H. Karlsen, I. Khushi, and T. P. Hagen, "Cost of extracorporeal membrane oxygenation: evidence from the rikshospitalet university hospital, oslo, norway," *European journal of cardio-thoracic surgery*, vol. 37, no. 2, pp. 339–342, 2010.

[6] D. A. Murphy, L. E. Hockings, R. K. Andrews, C. Aubron, E. E. Gardiner, V. A. Pellegrino, and A. K. Davis, "Extracorporeal membrane oxygenation—hemostatic complications," *Transfusion medicine reviews*, vol. 29, no. 2, pp. 90–101, 2015.

[7] C. I. Castro and J. C. Briceno, "Perfluorocarbon-based oxygen carriers: review of products and trials," *Artificial organs*, vol. 34, no. 8, pp. 622–634, 2010.

[8] B. D. Spiess, "Perfluorocarbon gas transport: an overview of medical history with yet unrealized potentials," *Shock*, vol. 52, no. 1S, pp. 7–12, 2019.

[9] C. Bialas, C. Moser, and C. A. Sims, "Artificial oxygen carriers and red blood cell substitutes: A historic overview and recent developments toward military and clinical relevance," *Journal of Trauma and Acute Care Surgery*, vol. 87, no. 1S, pp. S48–S58, 2019.

[10] I. P. Torres Filho, "Mini-review: Perfluorocarbons, oxygen transport, and microcirculation in low flow states: in vivo and in vitro studies," *Shock*, vol. 52, no. 1S, pp. 19–27, 2019.

[11] J. S. Jahr, N. R. Guinn, D. R. Lowery, L. Shore-Lesserson, and A. Shander, "Blood substitutes and oxygen therapeutics: a review," *Anesthesia & Analgesia*, vol. 132, no. 1, pp. 119–129, 2020.

[12] Q.-C. Li, J. Yu, C.-H. Jiang, H.-H. Zhu, K. Liu, and J.-C. Zhao, "Effects of perfluorooctane on the retina as a short-term and small amounts remnant in rabbits," *International journal of ophthalmology*, vol. 12, no. 3, p. 381, 2019.

[13] S. Sarkar, A. Paswan, and S. Prakas, "Liquid ventilation," *Anesthesia, essays and researches*, vol. 8, no. 3, p. 277, 2014.

[14] C. L. Leach, J. S. Greenspan, S. D. Rubenstein, T. H. Shaffer, M. R. Wolfson, J. C. Jackson, R. DeLemos, and B. P. Fuhrman, "Partial liquid ventilation with perflubron in premature infants with severe respiratory distress syndrome," *New England Journal of Medicine*, vol. 335, no. 11, pp. 761–767, 1996.

[15] R. B. Hirschl, S. Conrad, R. Kaiser, J. B. Zwischenberger, R. H. Bartlett, F. Booth, and V. Cardenas, "Partial liquid ventilation in adult patients with ards: a multicenter phase i-ii trial. adult plv study group." *Annals of surgery*, vol. 228, no. 5, p. 692, 1998.

[16] K. S. Staffey, R. Dendi, L. A. Brooks, A. M. Pretorius, L. W. Ackermann, K. Zamba, E. Dickson, and R. E. Kerber, "Liquid ventilation with perfluorocarbons facilitates resumption of spontaneous circulation in a swine cardiac arrest model," *Resuscitation*, vol. 78, no. 1, pp. 77–84, 2008.

[17] M. R. Wolfson and T. H. Shaffer, "Pulmonary applications of perfluorochemical liquids: ventilation and beyond," *Paediatric respiratory reviews*, vol. 6, no. 2, pp. 117–127, 2005.

[18] R. B. Hirschl, M. Croce, D. Gore, H. Wiedemann, K. Davis, J. Zwischenberger, and R. H. Bartlett, "Prospective, randomized, controlled pilot study of partial liquid ventilation in adult acute respiratory distress syndrome," *American journal of respiratory and critical care medicine*, vol. 165, no. 6, pp. 781–787, 2002.
[19] B. Cullis, M. Abdelraheem, G. Abrahams, A. Balbi, D. N. Cruz, Y. Frishberg, V. Koch, M. McCulloch, A. Numanoglu, P. Nourse *et al.*, "Peritoneal dialysis for acute kidney injury," *Peritoneal dialysis international*, vol. 34, no. 5, pp. 494–517, 2014.
[20] S. R. Carr, J. P. Cantor, A. S. Rao, T. V. Lakshman, J. E. Collins, and J. S. Friedberg, "Peritoneal perfusion with oxygenated perfluorocarbon augments systemic oxygenation," *Chest*, vol. 130, no. 2, pp. 402–411, 2006.
[21] X. Sun, Y. Zhang, G. Lei, Y. Guo, and J. Zhu, "An improved deadbeat predictive stator flux control with reduced-order disturbance observer for in-wheel pmsms," *IEEE/ASME Transactions on Mechatronics*, 2021.
[22] Y. Huang, F. Wang, A. Li, Y. Shi, and Y. Chen, "Development and performance enhancement of an overactuated autonomous ground vehicle," *IEEE/ASME Transactions on Mechatronics*, vol. 26, no. 1, pp. 33–44, 2020.
[23] D. Potnuru, S. Ch *et al.*, "Design and implementation methodology for rapid control prototyping of closed loop speed control for bldc motor," *Journal of Electrical Systems and Information Technology*, vol. 5, no. 1, pp. 99–111, 2018.
[24] J. Watton, *Fundamentals of fluid power control*. Cambridge University Press, 2009, vol. 10.

Mahsa Doosthosseini received her M.S. (2017) in Mechanical Engineering from the Pennsylvania State University, and her Ph.D. (2021) in Mechanical Engineering from the University of Maryland, College Park. She is currently a postdoctoral researcher at the University of Maryland and her research focuses on optimal experiment design, control, and mechatronics.

Kevin R. Aroom earned his B.S. (2005) and M.S. (2007) in Biomedical Engineering from the University of Maryland, and University of Texas at Austin, respectively. His areas of expertise include rapid prototyping and medical devices.

Majid Reza Aroom recieved his B.Sc (1984) from the Northeastern University, Boston Massachusetts, USA. He is a project engineer in Thermal Systems, and a Mechanical Engineering Faculty Specialist currently at the University of Maryland.

Melissa Culligan received her M.S. in Clinical Research Management from Drexel University. She is the Director of Clinical Research at the Division of Thoracic Surgery at The University of Maryland Medical Center, and a Nursing Science Ph.D. student at The University of Maryland School of Nursing.

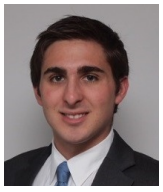

Warren Naselsky earned his B.S. in Biochemistry (2012) and M.D. (2016) at the University of North Carolina at Chapel Hill. He is currently an integrated cardiothoracic surgical resident at the University of Maryland. He recently completed an NIH T32 postdoctoral fellowship at the University of Maryland and now is pursuing a career as an academic thoracic surgeon.

Chandrasekhar Thamire holds a B.S. (1987), M.S. (1997), and Ph.D. (1997) degrees, all in mechanical engineering, and is a licensed engineer. His areas of expertise are turbomachinery design and biological transport. He has worked in industry and academia in various capacities. He is presently a principal lecturer at the University of Maryland.

Stephen A. Roller holds an MBA from the University of Minnesota Carlson School of Management and has his M.Sc. from the University of Michigan in Biomedical Engineering. He also holds his B.Sc. from the University of Michigan in Mechanical Engineering. He serves as a venture advisor with a focus on medical device technologies currently at the University of Maryland.

Richard Hughen earned his BS and MBA degrees from The Pennsylvania State University. He is currently CEO of a start-up company developing a predictive continuous respiratory monitoring device for the patient bedside and home. His main expertise is medical device commercialization and is an Entrepreneur in Residence for University of Maryland Ventures.

Henry W. Haslach, Jr earned a BS in mathematics from Trinity College, an MS in mathematics from the University of Chicago, an MS in Engineering Mechanics and a Ph.D in mathematics both from the University of Wisconsin-Madison. His current research and expertise are on the experimental and analytical rupture mechanics of the human aorta and on blast damage to the brain. He is currently a Research Professor in Mechanical Engineering at the University of Maryland – College Park.

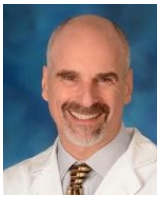

Joseph S. Friedberg is the Charles Reid Edwards Professor of Surgery and head of the Division of Thoracic Surgery at the University of Maryland School of Medicine. He received his bachelor's degree from the University of Pennsylvania, and received his M.D. from Harvard Medical School. His interests include pleural mesothelioma, pleural malignancies and disorders, complex lung cancer, chest wall tumors, pulmonary metastasis, malignant pleural effusions, and diaphragm disorders.

Jin-Oh Hahn received BS and MS degrees in mechanical engineering from Seoul National University in 1997 and 1999, and PhD degree in mechanical engineering from Massachusetts Institute of Technology (MIT) in 2008. He is currently with the University of Maryland, where he is an Associate Professor in the Department of Mechanical Engineering. His research interests include applications of control, estimation, and machine learning theory to health monitoring, fault diagnostics, maintenance and treatment of dynamical systems with emphasis on health and medicine.

Hosam K. Fathy earned his B.Sc. (1997), M.S. (1999), and Ph.D. (2003) degrees - all in Mechanical Engineering - from The American University in Cairo, Kansas State University, and The University of Michigan, respectively. His main area of expertise is optimal estimation and control. He is currently a Mechanical Engineering Professor at The University of Maryland.